Low energy scattering cross sections for $n + {}^{6,7}$Li reactions using the continuum-discretized coupled-channels method

D. Ichinkhorloo,[1,*] M. Aikawa,[2] S. Chiba,[3,4] Y. Hirabayashi,[5] and K. Katō[2]

[1]*Meme Media Laboratory, Hokkaido University, Sapporo 060-8628, Japan*
[2]*Nuclear Reaction Data Centre, Faculty of Science, Hokkaido University, Sapporo 060-0810, Japan*
[3]*Research Laboratory for Nuclear Reactors, Tokyo Institute of Technology, Tokyo 152-8550, Japan*
[4]*National Astronomical Observatory of Japan, Mitaka, Tokyo 181-8588, Japan*
[5]*Information Initiative Center, Hokkaido University, Sapporo 060-0811, Japan*

(Received 2 March 2016; revised manuscript received 3 May 2016; published 23 June 2016)

We study the integrated elastic and inelastic scattering cross sections together with their angular distributions of $n + {}^{6,7}$Li using $n+$ $(\alpha + d)$ and $n+$ $(\alpha + t)$ cluster models, respectively, and the continuum-discretized coupled-channel framework. The microscopic single-folding potential is used for the neutron energies from 1 to 24 MeV. The calculated elastic and inelastic scattering cross sections are in good agreement with experimental and evaluated data for the observed incident energies.

DOI: 10.1103/PhysRevC.93.064612

I. INTRODUCTION

The $n+$ Li reactions have attracted a lot of attention not only from the basic interest but also from the application point of view. Lithium isotopes will be used as a tritium-breeding material in $d - t$ fusion reactors. Therefore accurate nuclear data are required for n-induced reactions of ^{6,7}Li.

In the previous works [1–3], we have successfully studied cross sections for the $n + {}^{6,7}$Li elastic and inelastic scattering angular distributions and neutron spectra applying the continuum-discretized coupled-channel (CDCC) method [4] assuming $n+$ $(\alpha + d)$ and $n+$ $(\alpha + t)$ models. It was found that the calculated cross sections for incident energies from 7.47 to 24 MeV can be reproduced by their cluster models with one normalization factor for the imaginary part of the $n - {}^{6,7}$Li folding potential of the complex Jeukenne-Lejeune-Mahaux effective nucleon-nucleon (JLM) [5] interaction. More recently, Guo *et al.* [6] have analyzed both neutron and proton scatterings from ^{6,7}Li in a wide incident-energy range up to 150 MeV, and demonstrated the applicability of the CDCC to nucleon scattering from ^{6,7}Li. They analyzed neutron total cross sections, proton reaction cross sections, and differential cross sections of nucleon elastic and inelastic scatterings. However, it is still difficult to reproduce the data at energy lower than about 10 MeV in their frameworks.

In this work, we extend the CDCC analysis of the integrated elastic and inelastic scattering cross sections of $n + {}^{6,7}$Li with incident neutron energies below 14.1 MeV using the JLM which was proposed for an energy region lower than 10 MeV [7]. This is because of the fact that the different kinds of the parameter sets are defined for the JLM effective nucleon-nucleon interaction in lower and higher energy regions [5,7]. Furthermore, we employ the normalization factors to adjust the folding potentials of the JLM for the $n + {}^{6,7}$Li elastic scattering in a similar way as the previous studies [1–3]. The energy-dependent normalization factors λ_v and λ_w for real and imaginary parts, respectively, of the $n - {}^{6,7}$Li folding potentials are determined from the integrated elastic cross section data.

Using the obtained normalization factors, we calculate the inelastic scattering cross sections and angular distributions and compare the results with the experimental data without any additional parameters. Recently, a new experiment of the inelastic neutron scattering cross section to the first excited state in ^{7}Li was measured by Nyman *et al.* [8]. We discuss the comparison between the experimental, evaluated data and our CDCC calculations.

This paper is organized as follows. We describe the CDCC method including calculations of ^{6,7}Li wave functions and the $n - {}^{6,7}$Li folding potentials of the JLM interaction in Sec. II. We present the calculated results and discuss the applicability of the CDCC in Sec. III. Finally, we give a conclusion in Sec. IV.

II. THE MODEL AND METHOD

The Schrödinger equation of the $n + {}^{6,7}$Li scattering systems, which are described by using the $n+$ $(\alpha + c)$ three-body model with $c = d$ and t, is written as

$$\left[K_R + \sum_{i \in \alpha, c} v_{\rm in} + H({}^{6,7}\mathrm{Li}) - E \right] \Psi(\vec{r}, \vec{R}) = 0, \qquad (1)$$

where E is the energy of the total system, vectors $\vec{r}$ and $\vec{R}$ are the relative coordinates between α and c, and between the center of mass of the $\alpha - c$ pair and n, respectively. The operators $K_{\vec{R}}$ and $H({}^{6,7}\mathrm{Li})$ describe the kinetic energy associated with $\vec{R}$ and the Hamiltonian for $\alpha + c$. The second term, $\sum_{i \in \{\alpha, c\}} v_{\rm in}$ is the interaction between incident neutron and the ith nucleon in α and c clusters where $v_{\rm in}$ is an effective nucleon-nucleon interaction.

The total wave function $\Psi(\vec{r}, \vec{R})$ with the total angular momentum J and its projection M on the z axis is expanded in terms of the orthonormal set of eigenstates of $H({}^{6,7}\mathrm{Li})$

*Present address: Faculty of Science, Hokkaido University, Sapporo 060-0810, Japan; ichinkhorloo@nucl.sci.hokudai.ac.jp

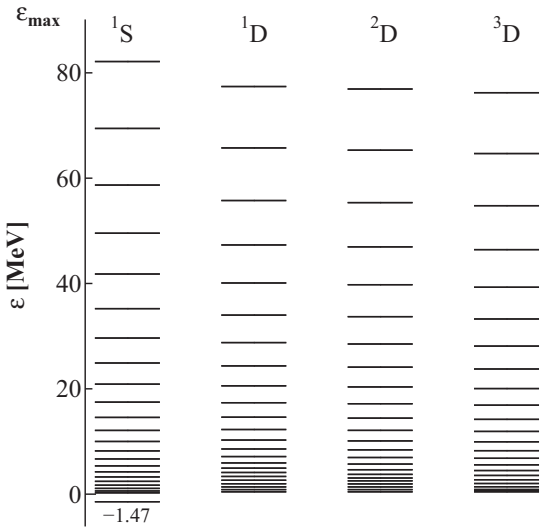

FIG. 1. The discretized eigenstates of ^{6}Li. Each panel indicated as ^1S,^1D,^2D, and ^3D, from left to right sides.

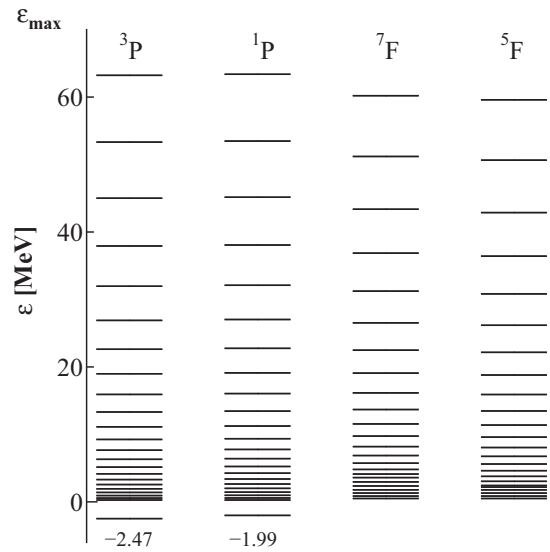

FIG. 2. The discretized eigenstates of ^{7}Li. Each panel indicated as ^3P,^1P,^7F, and ^5F, from left to right sides.

for the $\alpha + c$ system. The detailed explanations are given in Refs. [1–3].

For ^{6}Li, the binding energy of the 1^+ ground state is observed as -1.47 MeV with respect to the $\alpha + d$ threshold, and the $\alpha + d$ scattering phase shifts in the S wave ($\ell = 0$) and D wave ($\ell = 2$) have been obtained experimentally. The excited 3^+,2^+, and 1^+ states of ^{6}Li are observed at excitation energies of 2.18 MeV, 4.31, and 5.68 MeV, respectively, which are considered to be the triplet resonance states in the $\alpha + d$ model with the D wave. Level sequences of the discrete eigenstates of ^{6}Li are shown in Fig. 1. In the ^{7}Li case, the $3/2^-$ and $1/2^-$ bound states are observed at -2.47 MeV and -1.99 MeV ($\ell = 1$) with respect to the $\alpha + t$ threshold, respectively. The excited states of $7/2^-$ and $5/2^-$ are also observed at excitation energies of 4.65 MeV and 6.60 MeV, respectively, which are described by the present $\alpha + t$ cluster model with the F wave. Level sequences of the discrete eigenstates of ^{7}Li are shown in Fig. 2.

The observed bound state energies of ^{6,7}Li are well reproduced by the $\alpha + c$ cluster model, where $c = d$ and t for ^{6}Li and ^{7}Li, respectively. The bound and unbound states of ^{6,7}Li wave functions are expressed as

$$\hat{\phi}_{\ell I}(^{6,7}\mathrm{Li},\mathrm{b.s.}) = \varphi(\alpha)[\varphi_j(c) \otimes u_\ell(\mathrm{b.s.},\vec{r})]_I, \qquad (2)$$

and

$$\hat{\phi}_{\ell I}(^{6,7}\mathrm{Li},k) = \varphi(\alpha)[\varphi_j(c) \otimes u_\ell(k,\vec{r})]_I, \qquad (3)$$

respectively, where $\varphi(\alpha)$ and $\varphi_j(c)$ stand for the internal wave functions of the alpha cluster and the cluster c (deuteron or triton) with spin j, respectively. The relative wave functions $u_\ell(\mathrm{b.s.},\vec{r})$ and $u_\ell(k,\vec{r})$ of the relative coordinate $\vec{r}$ between α and c are given by the solutions of the orthogonality condition model (OCM) [9] in the same way as Ref. [4] with the complex Gaussian basis functions Ref. [10]. As for the interaction between α and c, we parametrized central and spin-orbit potentials ℓ dependently so as to reproduce the energies of the ground and excited states, and the $\alpha + c$ scattering phase shifts by a two-range Gaussian form and by a two-range Gaussian-derivative form, respectively. For the $\alpha + d$ system, the parameter values employed here are listed in Table I. For the $\alpha + t$ system, we use the same parameters as presented in the previous work [3]. As the discretization approach, we adopt the pseudostate method [11–13] in the CDCC framework and represent the ith discretized wave function as $\hat{\phi}_\gamma(^{6,7}\mathrm{Li})$ with $\gamma = (i\ell I)$. Discretized states included in the present calculation are shown in Figs. 1 and 2.

The diagonal and coupling potentials for $n + ^{6,7}$Li systems are calculated by folding the JLM effective nucleon-nucleon interaction in the same way as Ref. [3].

$$V_{\gamma,\gamma'}(\vec{R}) = \langle\hat{\phi}_\gamma(^{6,7}\mathrm{Li})| \sum_{i\in\{\alpha,c\}} v_{\mathrm{in}}|\hat{\phi}_{\gamma'}(^{6,7}\mathrm{Li})\rangle_{\vec{R}}. \qquad (4)$$

For incident energies higher than 10 MeV, the JLM potential parameters given in Ref. [5] is used as shown in our previous calculations [1–3]. On the other hand, for energies lower than

TABLE I. The parameters of the effective central and spin-orbit potentials between α and d for $\ell = 0$ and 2 in the ^{6}Li system. $V_\ell^{\mathrm{CE}}(r) = v_{1,\ell}e^{-(r/r_{1,\ell})^2} + v_{2,\ell}e^{-(r/r_{2,\ell})^2}$ $V_\ell^{\mathrm{SO}}(r) = v_{1,\ell}^{\mathrm{SO}}re^{-(r/r_{1,\ell})^2} + v_{2,\ell}^{\mathrm{SO}}re^{-(r/r_{2,\ell})^2}$.

Parameters	$\ell = 0$	$\ell = 2$
$v_{1,\ell}$(MeV)	-105.85	-82.98
$v_{2,\ell}$(MeV)	46.22	31.00
$v_{1,\ell}^{(\mathrm{SO})}$(MeV)	–	-2.31
$v_{2,\ell}^{(\mathrm{SO})}$(MeV)	–	1.42
$r_{1,\ell}$(fm)	2.191	2.377
$r_{2,\ell}$(fm)	1.607	1.852
$r_{1,\ell}^{(\mathrm{SO})}$(fm)	–	2.377
$r_{2,\ell}^{(\mathrm{SO})}$(fm)	–	1.852

10 MeV, we employ the different parameters of the JLM potential, which is discussed in Ref. [7].

III. RESULTS AND DISCUSSION

A. $n + {}^6$Li scattering

We analyze the integrated elastic and inelastic cross sections of the $n + {}^6$Li scattering. Here, we describe the inelastic resonant state of ^{6}Li using discrete basis functions in the CDCC framework. Because the resonant state has a distribution over an energy range of the resonance width Γ around the resonance energy E_r, we calculate the inelastic cross section of $n + {}^6$Li for a resonant state of ^{6}Li taking a sum of the breakup cross sections of $n+ (\alpha + d)$ for several discretized solutions obtained in the resonance energy region. In the $n + {}^6$Li scattering, we calculate the inelastic cross section for the 3^+ resonant state of ^{6}Li at the 2.18-MeV excitation energy by taking a sum of three solutions obtained around the resonance energy of the $\alpha + d$ system.

We first take the normalization factors $\lambda_v = 1.0$ and $\lambda_w = 0.2$ to reproduce the observed integrated elastic scattering cross sections data from 1 to 24 MeV as shown in Fig. 3, where the calculated results are presented by the dotted line (JLM-1). These values for λ_v and λ_w indicate that the small imaginary potential is needed while the real part has no adjustment parameter. This is almost consistent with $\lambda_v = 1.0$ and $\lambda_w = 0.1$ in the previous studies [1–3], and means that the CDCC framework of the $n+ (\alpha + d)$ model well describes the $n + {}^6$Li scattering. But we cannot reproduce experimental data of the lower incident neutron energy region for elastic scattering cross sections as shown in Fig. 3.

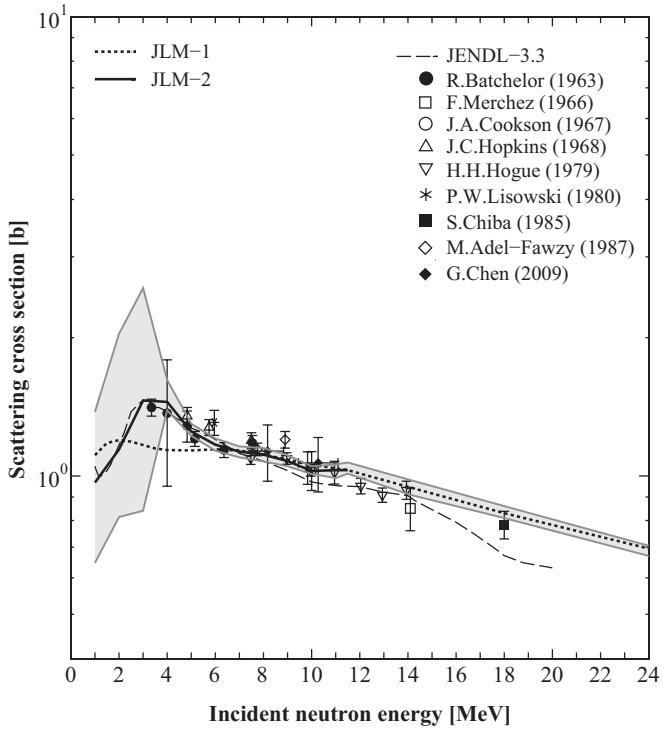

FIG. 3. The integrated elastic cross sections of the $n + {}^6$Li scattering, in comparison with the evaluated data [14] and experimental data [15–23].

TABLE II. The normalization factors λ_v and λ_w for real and imaginary parts, respectively, of the $n - {}^6$Li folding potential.

E_n (MeV)	λ_v	λ_w
1.0	1.256	0.0
2.0	1.277	0.0
3.0	1.242	0.0
4.0	1.235	0.0
5.0	1.160	0.0
6.0	1.120	0.0
7.0	1.060	0.1
8.0	1.060	0.1
9.0	1.040	0.15
10.0	1.030	0.2
11.0	1.020	0.2
$\geqslant$11.5	1.000	0.2

Second, we try to readjust normalization factors λ_v and λ_w so as to reproduce the low energy data of the measured integrated elastic cross section below 11.5 MeV. The obtained normalization factors for each energy are presented in Table II, and the calculated integrated elastic cross sections are shown by the solid line (JLM-2) in Fig. 3. As seen from Table II, λ_v for the real part of the potential becomes larger than 1.0 but the imaginary part λ_w goes to zero. The integrated elastic cross section is very sensitive to values of λ_v in lower energies. We indicate this sensitivity by the gray area in Fig. 3 where the upper and lower lines of the integrated elastic cross sections are calculated for $\lambda_v \pm 0.01$.

The energy dependence suggests a reason for effects from the resonance structure of the compound states in ^{7}Li which are excited during a colliding time of the low energy $n + {}^6$Li scattering. The incident energy $E_n = 10$ MeV corresponds to about 8.57-MeV excitation energy of the ^{7}Li system. In the excitation energy region lower than this energy of ^{7}Li, we observe several resonant states but not so many. These discrete resonant states may give a strong energy dependence on the $n + {}^6$Li scattering cross sections.

As shown in Fig. 3, it is noticed that the calculated integrated elastic cross sections show a good agreement with the evaluated data (JENDL-3.3) [14] for the $n + {}^6$Li scattering. After fixing the parameters of λ_v and λ_w, we try to calculate the integrated inelastic scattering cross section and angular distributions of the elastic and inelastic scattering to see the reliability of these parameter values.

We calculate the integrated inelastic cross sections for the 2.18 MeV state of ^{6}Li, and show the results together with the experimental data in Fig. 4. When we calculate them with an energy-independent normalization factors we obtain the result (JLM-1) of a fall-off behavior in lower energies, which show a large deviation from the observed data. On the other hand, the energy-dependent normalization factors bring about a very good result in comparison with the experimental data and the evaluation data of JENDL-3.3.

Using the same energy-dependent normalization factors, we calculate the angular distributions. Figure 5 shows the

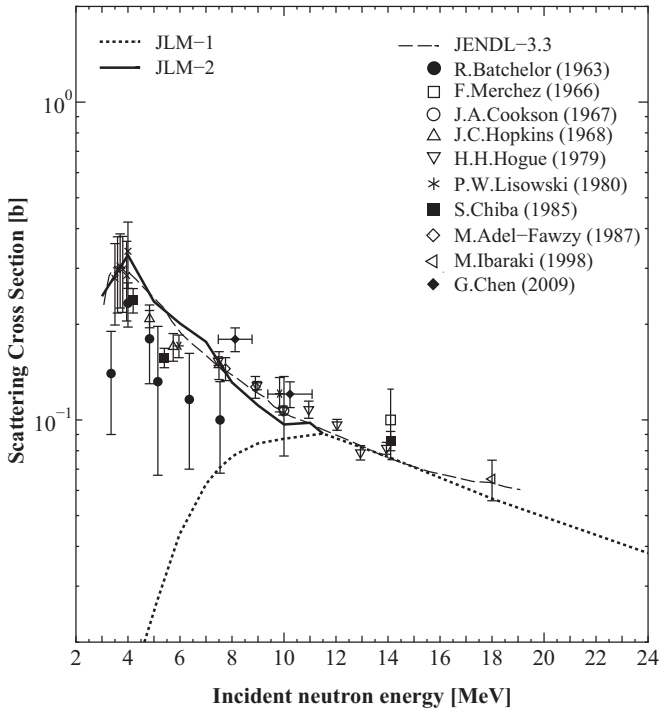

FIG. 4. The integrated inelastic $n + {}^{6}$Li scattering cross sections for the excited 3^{+} state at the excitation energy of 2.18 MeV of ^{6}Li in comparison with the evaluated data [14] and experimental data [15–25].

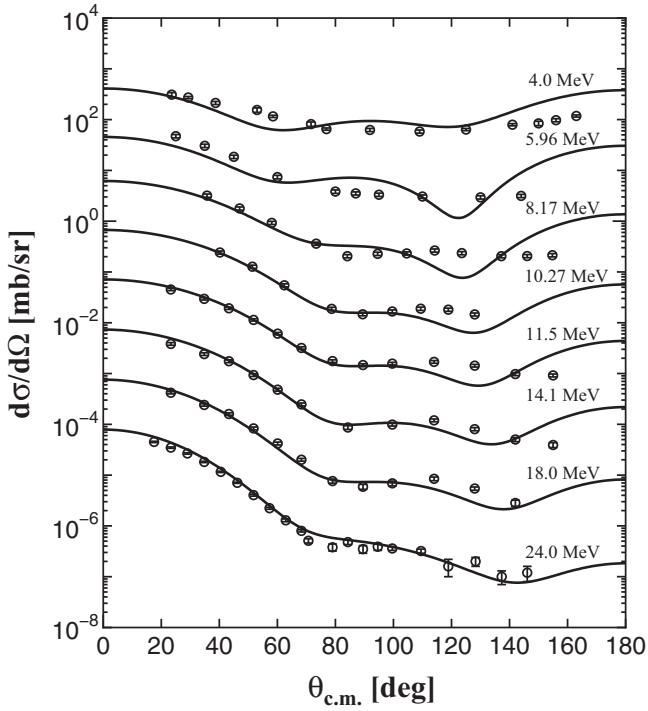

FIG. 5. Elastic angular distribution of the $n + {}^{6}$Li scattering for incident energies between 4.0 and 24.0 MeV. The solid lines and open circles correspond to the calculated results and experimental data [15,16,23,25–28], respectively. The data are subsequently shifted downward by a factor of $10^{-1}-10^{-7}$ from 5.96 to 24.0 MeV.

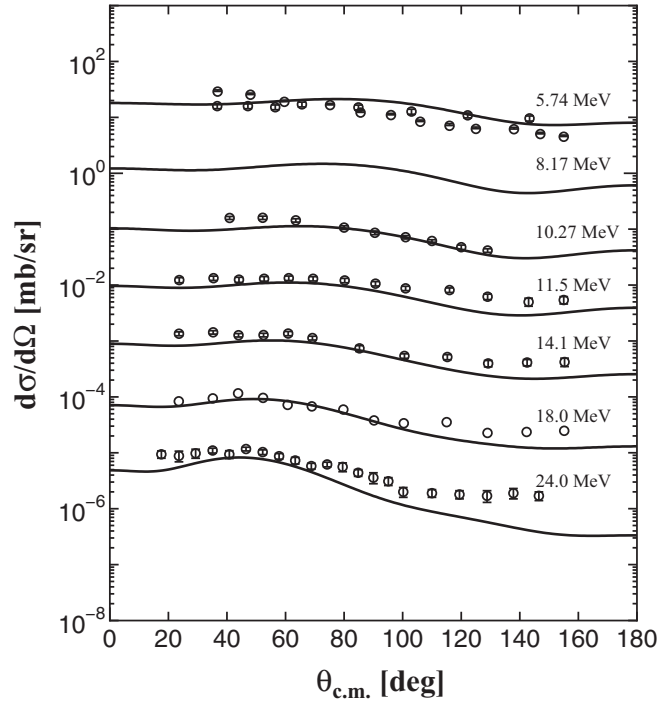

FIG. 6. Angular distributions of the $n + {}^{6}$Li inelastic scattering for the excited 3^{+} state at the excitation energy of 2.18 MeV of ^{6}Li. The solid lines and open circles correspond to the calculated results and experimental data [15,23,25,27–29], respectively. The data are subsequently shifted downward by a factor of $10^{-1}-10^{-6}$ from 8.17 to 24.0 MeV.

results of calculations and experiments of the differential cross sections of the $n + {}^{6}$Li elastic scattering with incident energies between 4.0 and 24.0 MeV. One can see that the results of the CDCC calculation represented with the solid line are in good agreement with the experimental data. For inelastic scattering, Fig. 6 shows the angular distributions to the 3^{+} resonance state of ^{6}Li, for incident neutron energies $E_n = 5.74, 7.5, 8.17, 10.27, 14.1, 18.0$, and 24.0 MeV. We see a good agreement in a wide energy region.

From these results, we can say that the CDCC calculations reproduce the observed inelastic cross sections together with the elastic ones using the same parameter values for λ_v and λ_w. This result indicates that the present CDCC calculations can successfully describe both elastic and inelastic scattering cross sections of $n - {}^{6}$Li over somewhat wide energies even lower than 10 MeV.

B. $n + {}^{7}$Li scattering

We also analyze the integrated elastic and inelastic scattering cross sections of the $n + {}^{7}$Li scattering at the incident neutron energy region from 1 to 24 MeV, in the same way as the $n + {}^{6}$Li scattering case. Because of the small energy difference (0.478 MeV) between the ground $(3/2^{-})$ and first-excited $(1/2^{-})$ states in ^{7}Li, it is difficult to separate those states in the final state of the $n + {}^{7}$Li scattering experimentally. To compare such experimental data, therefore, we calculate a sum of the cross sections of these two states as the elastic one.

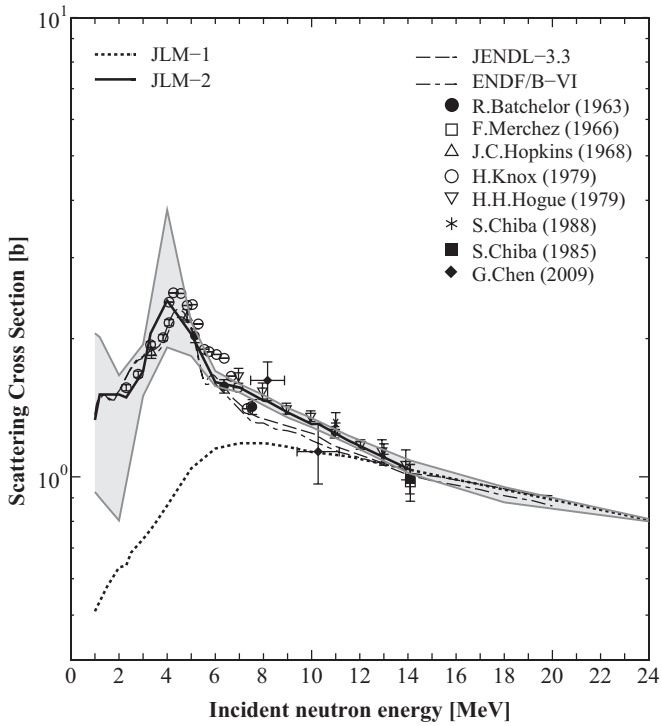

FIG. 7. The integrated elastic $n + {}^{7}$Li scattering cross sections, in comparison with the evaluated data [14,30] and experimental data [15,16,20–23,27,29].

For the $n + {}^{7}$Li elastic scattering of the neutron incident energies from 1 to 24 MeV, we take the normalization factors $\lambda_v = 1.0$ and $\lambda_w = 0.2$. The calculated elastic cross sections are presented by the dotted line (JLM-1) in Fig. 7. The imaginary potential is very small as well as the $n + {}^{6}$Li case, and the calculated result shows a good agreement with the evaluated data JENDL-3.3 [14] and ENDF/B-VI [30] in the energy region higher than 14.1 MeV where there are no experimental data. However, the calculated one below 11.5 MeV falls off much faster than the experimental data [15,16,20–23,27,29].

In the same way as the $n + {}^{6}$Li scattering, we adjust the normalization factor λ_v at each incident energy below $E_n = 11.5$ MeV assuming $\lambda_w = 0$. The obtained values of λ_v and λ_w are presented in Table III including those for $E_n \geqslant 14.1$ MeV, and calculated elastic cross sections are shown by the solid line (JLM-2) in Fig. 5. Values of λ_v are slightly larger than 1.0, and their energy dependence is considered to be owing to the formation of compound states of $n + {}^{7}$Li as was discussed in the $n + {}^{6}$Li case. It is also seen that the integrated elastic cross section is very sensitive to values of λ_v in lower energies as shown by the gray area bounded by upper and lower lines calculated for $\lambda_v \pm 0.01$.

Although the above elastic cross section includes the first excited state of ^{7}Li in addition to the ground state, there are many experiments which have measured the γ-ray production cross sections for 478-keV $(1/2^- \rightarrow 3/2^-_{\text{g.s.}})$ transition in ^{7}Li following inelastic neutron scatterings. Recently, Nyman *et al.* [9] reported the new data comparing with previous observations. However, there is no theoretical calculation so far. In our CDCC framework with the $n - {}^{7}$Li folding potential fitted to the elastic cross section, it is easy to calculate the inelastic cross section for the first excited $1/2^-$ state at 478 keV with two kinds of the parameter set (JLM-1 and JLM-2). The results are shown in Fig. 8 and compared with experimental data including the recent new data [8]. The JLM-1 calculation is an underestimation and shows the fall-off behavior in the energy region lower than 7 MeV, but the JLM-2 calculation successfully reproduces the experimental data increasing in the low energy region. Especially the peak of cross section around 4 MeV is well explained by the JLM-2 calculation.

TABLE III. The normalization factors λ_v and λ_w for real and imaginary parts, respectively, of the $n - {}^{7}$Li folding potential.

E_n (MeV)	λ_v	λ_w
1.0	1.155	0.0
1.2	1.160	0.0
2.0	1.165	0.0
2.3	1.165	0.0
3.0	1.165	0.0
4.0	1.150	0.0
5.0	1.120	0.0
6.0	1.060	0.0
7.0	1.040	0.0
8.0	1.040	0.0
9.0	1.040	0.0
10.0	1.040	0.0
11.5	1.000	0.1
$\geqslant$14.1	1.000	0.2

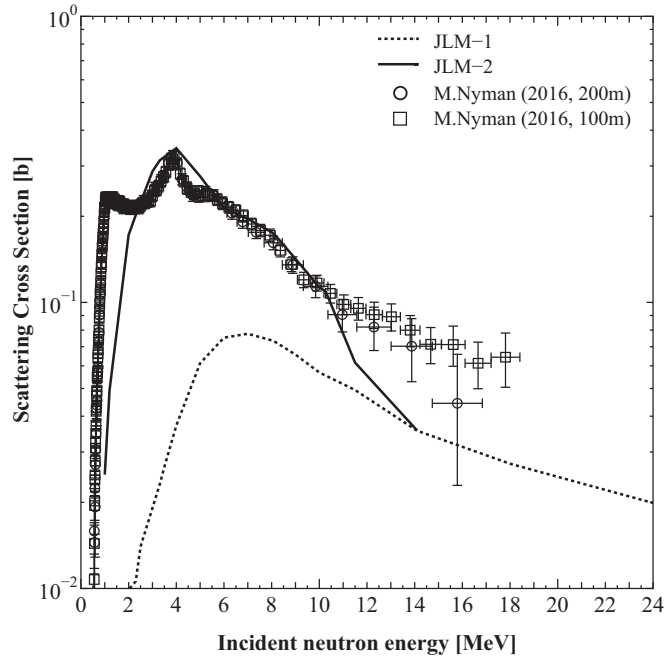

FIG. 8. The integrated inelastic $n + {}^{7}$Li scattering cross sections for the excited $1/2^-$ state at the excitation energy 478 keV of ^{7}Li with experimental data [8].

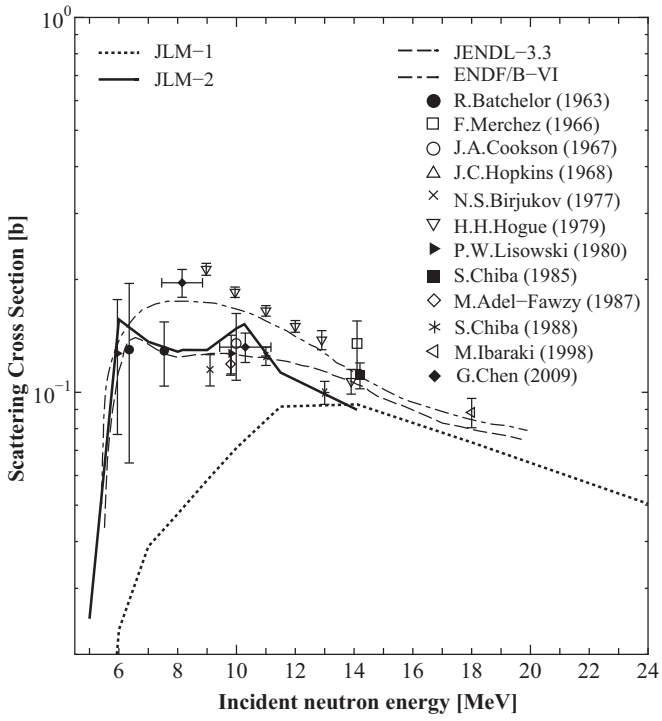

FIG. 9. The integrated inelastic $n + {}^{7}$Li scattering cross sections for the excited $7/2^-$ state at the excitation energy of 4.65 MeV of ^{7}Li, in comparison with the evaluated data [14,30] and experimental data [15–23,25,27,29].

However, the JLM-2 calculation falling down rapidly cannot reproduce another peak at low energies.

Figure 9 we calculate the other integrated inelastic cross section for the 4.65-MeV ($7/2^-$) state of ^{7}Li. In the neutron incident energies from 8 to 14 MeV, we see two groups of experimental data [15–23,25,27,29]; one group is almost flat but another one increases with decreasing of the energy. The evaluation data are also separated into two groups: The JENDL-3.3 [14] supports the former data but the ENDF/B-VI [30] suggests the latter behavior. Our calculations of the JLM-2 show the consistency with the latter data, although the JLM-1 calculation falls off rapidly as the energy decreases.

Using the JLM-2 parameters, we calculate the angular distributions of the elastic cross section where the inelastic ones to the first excited state are included as well. The obtained results are presented in Fig. 10 together with the experimental data for the incident energies from 2.3 to 24.0 MeV [15,23,27–29]. The calculated results are in reasonable agreement with the experimental data. For the inelastic scattering to the $7/2^-$ resonant state of ^{7}Li, Fig. 11 shows the angular distributions of energies from $E_n = 8.17$ to 24 MeV. Here we calculate differential cross sections of the inelastic scattering for the $7/2^-$ resonant state by taking a sum of the breakup cross section to five discretized $7/2^-$ solutions obtained around the resonance energy. From Fig. 11, we can see that the CDCC calculation with the JLM-2 can also reproduce the inelastic observed cross sections together with the elastic ones.

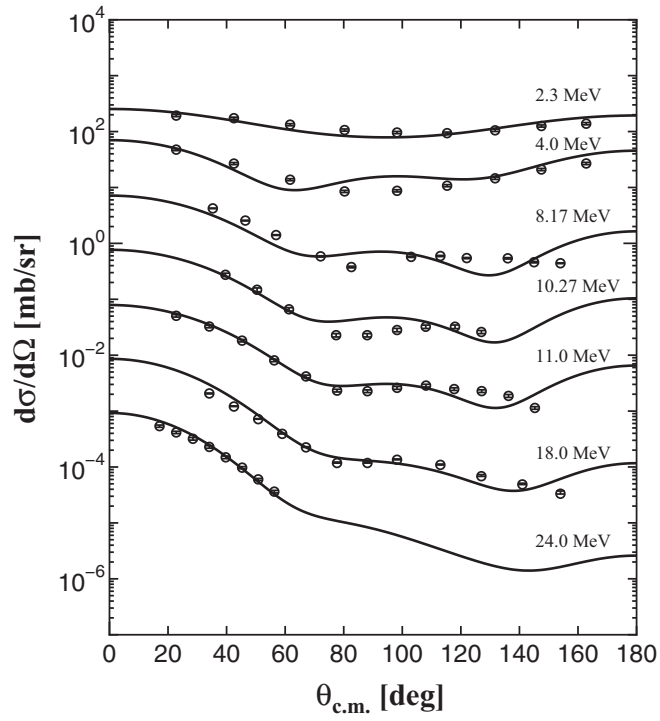

FIG. 10. Elastic angular distribution of the $n + {}^{7}$Li scattering for incident energies between 2.3 and 24.0 MeV. The solid lines and open circles correspond to the calculated results and experimental data [15,23,27–29], respectively. The data are subsequently shifted downward by a factor of $10^{-1}-10^{-6}$ from 4.0 to 24.0 MeV.

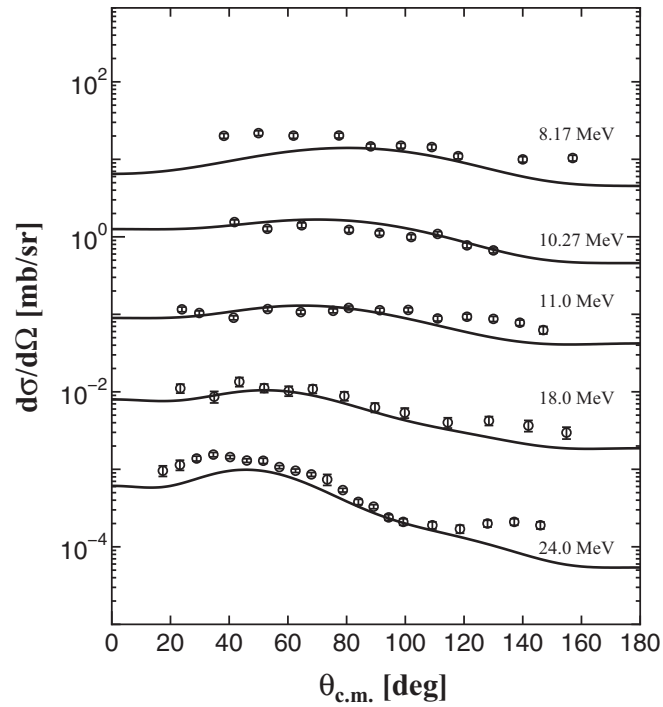

FIG. 11. Angular distributions of the $n + {}^{7}$Li inelastic scattering for the excited $7/2^-$ state at the excitation energy of 4.65 MeV of ^{7}Li. The solid lines and open circles correspond to the calculated results and experimental data [15,23,27,28], respectively. The data are subsequently shifted downward by a factor of $10^{-1}-10^{-4}$ from 10.27 to 24.0 MeV.

IV. CONCLUSION

Using the CDCC framework of the $n+(\alpha+d)$ and $n+(\alpha+t)$ models, we investigated the integrated elastic and inelastic scattering cross sections for ^{6,7}Li at incident neutron energies from 1 to 24 MeV using the $n+^{6,7}$Li folding potentials with two kinds of the complex-JLM effective nucleon-nucleon interactions [5,7] for higher and lower energy regions. We introduce the normalization factors for real and imaginary parts of these folding potentials comparing with the observed elastic cross sections of the $n+^{6,7}$Li scattering. The energy independent (JLM-1) and dependent (JLM-2) normalization factors are examined for integrated elastic and inelastic cross sections and angular distributions.

The JLM-2 calculations, in which the energy-dependent normalization factors are determined so as to reproduce the elastic cross section of the whole energy region from 1 to 24 MeV, show a satisfactorily good agreement with the experimental data of inelastic cross sections and angular distributions. From these results, it is concluded that the CDCC calculations of JLM-2 can explain the experimental data of the integrated inelastic cross sections and angular distributions for the $n+^{6,7}$Li scattering cross sections consistently with the integrated elastic cross sections.

The application of the CDCC to the low-energy scattering is still an open problem, because assumptions of the CDCC may be too simple for low energy scattering. In the CDCC calculations, rearrangement channels and the antisymmetriztion between nucleons in projectile and target nuclei are neglected. Furthermore, the $\ell \cdot s$ interaction between incident neutron and target nucleus is not included in the present calculation. For these problems, we here tried to investigate the low energy scattering of $n+^{6,7}$Li by introducing a single parameter of the normalization factor for the folding potential based on the effective nucleon-nucleon interaction (JLM). The successful results of the present approach are very promising for more detailed studies of the CDCC in the low energy scattering.

ACKNOWLEDGMENTS

We would like to thank the members of the nuclear theory group at Hokkaido University and Dr. Markus Nyman and his experimental group of Institute for Reference Materials and Measurements, Belgium. This work was supported by "R&D Platform Formation of Nuclear Reaction Data in Asian Countries (2010–2013)," Asia-Africa Science Platform Program, and Grant-in-Aid for Publication of Scientific Research Results (Grant No. 257005), Japan Society for the Promotion of Science. M.A. and K.K. also thank the International Collaboration of the Al-Farabi Kazakh National University (Grants No. 3106/GF4 and No. 1550/GF3) for support.

[1] T. Matsumoto, D. Ichinkhorloo, Y. Hirabayashi, K. Katō, and S. Chiba, Phys. Rev. C **83**, 064611(R) (2011).
[2] D. Ichinkhorloo, Y. Hirabayashi, K. Katō, T. Matsumoto, and S. Chiba, J. Nucl. Sci. Technol. **48**, 1357 (2011).
[3] D. Ichinkhorloo, Y. Hirabayashi, K. Katō, M. Aikawa, T. Matsumoto, and S. Chiba, Phys. Rev. C **86**, 064604(R) (2012).
[4] M. Kamimura, M. Yahiro, Y. Iseri, Y. Sakuragi, H. Kameyama, and M. Kawai, Prog. Theor. Phys. Suppl. **89**, 1 (1986); Y. Sakuragi, M. Yahiro, and M. Kamimura, Prog. Theor. Phys. **89**, 136 (1986).
[5] J.-P. Jeukenne, A. Lejeune, and C. Mahaux, Phys. Rev. C **16**, 80 (1977).
[6] H. Guo, Y. Watanabe, T. Matsumoto, K. Ogata, and M. Yahiro, Phys. Rev. C **87**, 024610 (2013).
[7] A. Lejeune, Phys. Rev. C **21**, 1107 (1980).
[8] M. Nyman, F. Belloni, D. Ichinkhorloo, E. Pirovano, A. J. M. Plompen, and C. Rouki, Phys. Rev. C **93**, 024610 (2016).
[9] S. Saito, Prog. Theor. Phys. Suppl. **62**, 11 (1977).
[10] E. Hiyama, Y. Kino, and M. Kamimura, Prog. Part. Nucl. Phys. **51**, 223 (2003).
[11] A. M. Moro, J. M. Arias, J. Gómez-Camacho, I. Martel, F. Pérez-Bernal, R. Crespo, and F. Nunes, Phys. Rev. C **65**, 011602(R) (2001).
[12] T. Matsumoto, T. Kamizato, K. Ogata, Y. Iseri, E. Hiyama, M. Kamimura, and M. Yahiro, Phys. Rev. C **68**, 064607 (2003).
[13] T. Egami, K. Ogata, T. Matsumoto, Y. Iseri, M. Kamimura, and M. Yahiro, Phys. Rev. C **70**, 047604 (2004).
[14] K. Shibata, T. Kawano, T. Nakagawa, O. Iwamoto, J. Katakura, T. Fukahori, S. Chiba, A. Hasegawa, T. Murata, H. Matsunobu, T. Ohsawa, Y. Nakajima, T. Yoshida, A. Zukeran, M. Kawai, M. Baba, M. Ishikawa, T. Asami, T. Watanabe, Y. Watanabe, M. Igashira, N. Yamamuro, H. Kitazawa, N. Yamano, and H. Takano, Japanese Evaluated Nuclear Data, Library Version 3 Revision-3: JENDL-3.3, J. Nucl. Sci. Technol. **39**, 1125 (2002).
[15] G. Chen, X. Ruan, Z. Zhou, J. Zhang, B. Qi, X. Li, H. Huang, H. Tang, Q. Zhong, J. Jiang, B. Xin, J. Bao, and L. Chen, Nucl. Sci. Eng. **163**, 272 (2009).
[16] H. H. Hogue *et al.*, Nucl. Sci. Eng. **69**, 22 (1979).
[17] P. W. Lisowski *et al.*, Report No. LA-8342 (Los Alamos Scientific Laboratory, Los Alamos, 1980).
[18] J. A. Cookson *et al.*, J. Nucl. Phys. A **91**, 273 (1967).
[19] M. Adel-Fawzy *et al.*, Nucl. Instrum. Methods **169**, 533 (1980).
[20] R. Batchelor *et al.*, J. Nucl. Phys. **47**, 385 (1963).
[21] J. C. Hopkins *et al.*, J. Nucl. Phys. A **107**, 139 (1968).
[22] F. Merchez *et al.*, J. Phys. Colloque **27**, 1, 61 (1966).
[23] S. Chiba *et al.*, J. Nucl. Sci. Technol. **25**, 2, 210 (1985).
[24] N. S. Biryukov, B. V. Zhuravlev, N. V. Kornilov, V. I. Popov, A. P. Rudenko, O. A. Salnikov, and V. I. Trykova, At. Energ. **43**, 1787 (1977).
[25] M. Ibaraki *et al.*, JAERI-Research Report No. 98-032 (Japan Atomic Energy Research Institute, Ibaraki, 1998).
[26] A. B. Smith *et al.*, Nucl. Phys. A **373**, 305 (1982).
[27] S. Chiba, M. Baba, N. Yabuta, T. Kikuchi, M. Ishikawa, N. Hirakawa, and K. Sugiyama, in *Proceedings of the International Conference on Nuclear Data for Science and Technology* (Mito, 1988), p. 253.
[28] L. F. Hansen, J. Rapaport, X. Wang, F. A. Barrios, F. Petrovich, A. W. Carpenter, and M. J. Threapleton, Phys. Rev. C **38**, 525 (1988).
[29] H. Knox and R. O. Lane, J. BAP **23**, 942(DC2), 7811.
[30] Cross Section Evaluation Working Group, ENDF/B-VI Summary Documentation, Report BNL-NCS-17541 (ENDF-201) (Brookhaven National Laboratory, Upton, 1991).